Spatially varying finite-amplitude wave trains on falling liquid films

B. Gjevik

In a previous paper the occurrence of steady finite-amplitude waves on falling liquid films has been studied by a long wave expansion technique. This analysis is now extended to include spatially varying wave trains. The solutions presented may correspond to the forced wave trains occurring downstream from a wave generator. Moreover the second order terms in the long wave expansion are reported and their effect on the finite-amplitude wave motion is studied. Numerical results for finite-amplitude waves on thin films of water or alcohol are presented.

1. Introduction.

In a previous study, Gjevik [1] hereafter referred to as (I), the occurrence of finite-amplitude surface waves on falling liquid films has been investigated. However, this study is concerned with temporally growing or decaying wave solutions which are assumed to be periodic in the distance along the inclined plane. Therefore the transient development of these waves will correspond to special experimental arrangements and the solutions given in (I) will for example not explicitly provide any information about the spatial development of a steady wave train downstream from a wave generator. Since this latter arrangement is used by different authors [2,3] in order to study steady finite-amplitude surface waves on falling liquid films it might be pertinent to modify the analysis in (I) according to these experimental conditions. Mathematically these modifications merely consist of an interchange of the roles of time and distance downstream and the roles of wave number and frequency. It should be pointed out that generally there will exist a complex perturbation velocity field close to the wave generator and the kinetic energy will be distributed among the different eigen-modes and within a certain band in the frequency spectrum. For the range of the flow parameters of interest here only the surface mode treated in our work is unstable according to linearized stability theory, while all the other eigen-modes are rapidly damped. (Ref. 4). It is also reasonable to assume that the fundamental finite-amplitude wave components have a similar stabilizing effect on sideband wave perturbations as the

stabilizing effect shown by Eckhaus [5] for finite-amplitude disturbance to parallel flow between rigid planes. Therefore, the solution presented below might approximate the experimental disturbances at a point somewhat downstream from the wave generator. This position we shall refer to as the boundary station. In this work we shall also report the second order approximation to the long wave expansion (hereafter written LWE) which was found in (I) to be a convenient method for the study of long surface waves on thin falling liquid films. It was mentioned in (I) that although the higher order terms in the LWE would have a negligible influence on the computed wave amplitudes, these terms would have a significant effect on the velocity of the steady finite-amplitude wave. Consequently, these terms will also have an influence on the phase angle between the fundamental wave component and its higher harmonics.

2. Second order terms in long wave expansion including the effect of surface tension.

We shall consider two-dimensional perturbations to a steady parallel flow of an incompressible viscous fluid down an inclined plane and adopt the same notation and scaling procedure as introduced in (I). The flow is then characterized by a Reynolds number, a Weber number and the angle of inclination of the plane defined respectively by

$$R = \frac{gh^3 \sin\theta}{2\nu^2} , \tag{1a}$$

$$W = \frac{T}{\rho g h^2 \sin\theta} \tag{1b}$$

$$\theta , \tag{1c}$$

where g is the acceleration of gravity, h is a mean thickness of the fluid layer defined by the normalization condition imposed in § 4, ν is the kinematic viscosity, ρ is the density of the fluid and T denotes the surface tension. As in (I) we assume R to be of order unity. The surface deflection is a function of x and t which can be written (when scaled by h) :

$$\zeta(x,t) = 1 + \eta(x,t) \tag{2}$$

where $\eta(x,t)$ is a small perturbation of order $0(\varepsilon) << 1$, x is the distance along the flow direction and t is time. Since we assume no mass transport through the free surface nor through the bottom plane

$$\frac{\partial \zeta}{\partial t} = - \frac{\partial Q_x}{\partial x} , \tag{3}$$

where Q_x is the volume flux (pr. unit span) in the x-direction. With the LWE method as used in (I) the second order terms in Q_x can be evaluated. Hence if α denotes the expansion parameter

$$\begin{aligned} Q_x = A(\zeta) &+ \alpha\left(B(\zeta)\frac{\partial \zeta}{\partial x} + C(\zeta)\frac{\partial^3 \zeta}{\partial x^3}\right) \\ &+ \alpha^2\left(D(\zeta)\left(\frac{\partial \zeta}{\partial x}\right)^2 + E(\zeta)\,\frac{\partial^2 \zeta}{\partial x^2} + F(\zeta)\frac{\partial^4 \zeta}{\partial x^4}\right. \\ &\left. + G(\zeta)\frac{\partial \zeta}{\partial x}\,\frac{\partial^3 \zeta}{\partial x^3} + H(\zeta)\left(\frac{\partial^2 \zeta}{\partial x^2}\right)^2 + I(\zeta)\left(\frac{\partial \zeta}{\partial x}\right)^2\,\frac{\partial^2 \zeta}{\partial x^2}\right) , \end{aligned} \tag{4}$$

where the functions A, B, C etc. are defined in the Appendix. The fact that the equation for the surface deflection always can be written in form (3) to any order in the LWE for Q_x was apparently overlooked by Benney [6] and due to calculation errors

the equation for the surface deflection given in his paper cannot be transformed to (3). The last four terms in the expression (4) includes the effect of the surface tension and are to our knowledge not reported in earlier work on the subject. The corresponding second order approximation to the velocity field is given by lengthy algebraic expressions and will therefore be omitted here. The second order terms for the velocity field imply, however, a distortion of the mean velocity profile of order $0\ (\varepsilon^2\alpha^2)$. The distortion of the mean velocity profile is therefore obviously a negligible effect in establishing steady finite-amplitude wave motion on falling liquid films.

3. The amplitude equations for a spatially varying wave train.

We assume $\eta(x,t)$ to be a periodic function of t. Thus $\eta(x,t)$ can be expanded in a Fourier series

$$\eta(x,t) = \sum_{k=-N}^{k=N} A_k(x) e^{ikct} \quad , \tag{5}$$

where c is the dimensionless frequency scaled according to (I) by $\frac{\alpha g h \sin\theta}{2\nu}$. The Fourier coefficients A_k are functions of x and $A_{-k} = \overset{*}{A}_k$, where asterisk denotes complex conjugate and N denotes the number of terms retained in the Fourier series. We also write

$$A_k(x) = \tilde{A}_k(x) e^{ikx} \quad , \tag{6}$$

where α is the dimensionless wave number. Up to this stage α

is left unspecified. For a steady periodic wave train $\tilde{A}_k$ is independent of x. This case corresponds to the steady wave solutions given in (I). For a steady wave train and in a certain range of the flow parameters the result in (I) shows that the Fourier expansion will converge rapidly. If we are close to this steady state $\tilde{A}_k(x)$ will be a slowly varying function of x. Consequently we introduce the expansion (5) with $N = 2$ in the equation for the surface deflection (Eq.3). Moreover if only the first order derivatives of $\tilde{A}_k(x)$ $(k = 1,2)$ are retained, the following truncated set of amplitude equations is obtained.

$$a_1 \frac{d\tilde{A}_1}{dx} = (\beta_1 - ic)\tilde{A}_1 + q\tilde{A}_2\tilde{A}_1 + m|\tilde{A}_1|^2\tilde{A}_1 + r\tilde{A}_1\tilde{A}_0, \tag{7a}$$

$$a_2 \frac{d\tilde{A}_2}{dx} = (\beta_2 - 2ic)\tilde{A}_2 + p\tilde{A}_1^2. \tag{7b}$$

It also becomes evident from the further development (see Eq.9) that by a proper normalization of ζ the maximum value of $\tilde{A}_0$ will be of order $|\tilde{A}_1|^2$. Hence the term $\tilde{A}_1\tilde{A}_0$ should be retained in (7a). The coefficients in Eqs. (7a) and (7b) are given in the Appendix.

We now denote the mean value of a property of fluid with respect to t with a bar. Then from Eq. (3) it follows that

$$\bar{Q}_x = Q_0 \tag{8}$$

where Q_0 is determined by the conditions at the boundary station as defined in § 1. Thus our present formulation of the problem implies that the volume flux is periodic in time and has a mean value which is constant in the downstream direction. By a

substitution of (5) and (6) into (4), (8) can be written with a sufficient degree of accuracy as

$$\tfrac{2}{3} + 2\tilde{A}_0 + 4|\tilde{A}_1|^2 = Q_0$$

or equivalently

$$\tilde{A}_0 = \tfrac{1}{2}Q_0 - \tfrac{1}{3} - 2|\tilde{A}_1|^2. \qquad (9)$$

Hence (7a), (7b) and (9) form a complete set of equations and $\tilde{A}_1$, $\tilde{A}_2$ and $\tilde{A}_0$ are uniquely determined by the conditions imposed at the boundary station.

4. Steady far-field solutions of the amplitude equations.

In the range of the flow parameters leading to x-independent far-field solutions of (7a) and (7b) ζ can be normalized so that $\tilde{A}_0 = 0$ in the far-field range. This normalization defines the scaling parameter h as the mean film thickness in the far-field limit. Consequently (7a) and (7b) become analogous to the time-dependent amplitude equations studied in (I) and the steady far-field solution of (7a) and (7b) must correspond to the steady finite-amplitude wave solutions given in (I). There will be no loss in generality by choosing the origin of x so that for the far-field non-zero solutions we have

$$\tilde{A}_1 = B_1^{(s)}, \qquad (10a)$$

$$\tilde{A}_2 = B_2^{(s)} e^{i\Delta_1^{(s)}}, \qquad (10b)$$

where $B_1^{(s)}$, $B_2^{(s)}$ and $\Delta_1^{(s)}$ are real values independent of x.

Substitution of (10a) and (10b) in (7a) and (7b) leads to

$$B_1^{(s)} = (-\frac{\beta_{1r}}{P_r})^{\frac{1}{2}}, \quad \text{if} \quad \frac{\beta_{1r}}{P_r} > 0, \tag{11a}$$

$$B_2^{(s)} = -\frac{p_r\cos\Delta_1+p_i\sin\Delta_1}{\beta_{2r}} B_1^2, \quad \text{if} \quad \beta_{2r} \neq 0, \tag{11b}$$

$$tg\Delta_1^{(s)} = \frac{\beta_{2r}p_i-(\beta_{2i}-2\beta_{1i})p_r}{\beta_{2r}p_r+(\beta_{2i}-2\beta_{1i})p_i} \tag{11c}$$

where the indices r or i denote respectively the real or the imaginary part of a complex valued quantity and

$$P_r = \frac{16}{\beta_{2r}} + O(\alpha). \tag{12}$$

The following relation between wave amplitude and frequency must also be satisfied

$$c = \beta_{1i} + P_i B_1^{(s)^2}, \tag{13}$$

where

$$P_i = -2 + 4\frac{p_r+q_r}{\beta_{2r}} - 16\frac{\beta_{2i}-2\beta_{1i}}{\beta_{2r}^2} + O(\alpha^2). \tag{14}$$

With Eq. (13) also the dimensionless wave-number, α, of the far-field waves is determined. It follows from Eqs. (11a) and (12) that steady non-zero far-field solutions to (7a) and (7b) only exist for a certain band of frequencies. For relatively high frequencies leading to $\beta_{1r} < 0$ it is easily shown that (7a) and (7b) only possess the trivial solution $\tilde{A}_1$ & $\tilde{A}_2 \to 0$ for $x \to \infty$. On the other hand, for relatively low frequencies so that $|\beta_{2r}|$ becomes small compared to β_{1r}, the convergence of the series expansion, Eq. (5), will be violated. (See I). In the case of

non-dispersive infinitesimal-amplitude waves ($\beta_{2i} = 2\beta_{1i}$) the formulas (11a)-(11c) reduce to Eq. (22) in (I). Therefore the main effect of the second order terms in the LWE will be a correction to the angle Δ_1. The limit $\Delta_1 = \frac{\pi}{2}$ for $\alpha \to 0$. derived in (I) is, however, unaffected. For the case $\theta = \frac{\pi}{2}$ and for relatively short waves we found in (I) that the non-linear terms would lead to a negligible decrease in wave velocity i.e. for $\alpha^2 > 0.673\ R/W$. Since $\beta_{2i} - 2\beta_{1i}$ is negative for values of α and R within the range of non-zero far-field solutions to (7a) and (7b) (the case $R \ll 1$ excepted) it follows from Eqs. (13) and (14). that the dispersion terms will accentuate the velocity decrease in certain ranges of α and R. (See also numerical results in Table 1 and Table 2). For relatively longer waves the numerical results indicate that the non-linear terms lead to a weak increase in the wave velocity. In Lin's study of the steady wave solution the dispersion terms are neglected (See I). Therefore the velocity decrease for relatively short finite-amplitude waves was not shown in his previous analysis.[7] However, these results have been modified recently [Lin (1970) private communication]. It follows from the results in (I) that in the neighbourhood of the linear neutral line in the stability diagram the third harmonics $\tilde{A}_3$ will be negligible compared to $\tilde{A}_2$ and $\tilde{A}_1$ and a good approximation to the far-field wave amplitudes is found from Eq. (11). Since the third harmonic was included in the numerical calculations of the steady solution presented in (I), we have also included $\tilde{A}_3$ in the recalculations which admit the improvement in the LWE. Consistent with the definitions in (I)

we have introduced $\tilde{A}_3 = B_3^{(s)} e^{i(\Delta_2^{(s)} \mp \Delta_1^{(s)})}$, and we have solved a similar set of equations as Eq (15) in (I). The details in these numerical calculations are as described in (I). For small values of α and R the correction to the amplitudes $B_1^{(s)}$, $B_2^{(s)}$ and $B_3^{(s)}$ due to the second order terms in the LWE are almost negligible. But there is a considerable correction to the wave velocity as well as to the values of $\Delta_1^{(s)}$ and $\Delta_2^{(s)}$. The correction to these angles will have some influence on the wave profils given in (I), but the waves are still found to retain their characteristic shape with steep fronts and somewhat flatter valleys. The data for the far-field waves on a water film are given in Table 1 and Table 2 for two different angles of inclination, $\theta = \frac{\pi}{24}$ and $\theta = \frac{\pi}{2}$. The data in Table 2 are computed for the same values of the flow parameters as used in (I). The data in Table 1 are typical for some of Koehler's experiments [3] (quoted in § 5).

With the same method as described above we have also computed the far-field wave amplitudes for the values of the wave length, λ, and the mean volume flux corresponding to observed onset of wave motion on vertically falling films as reported by Kapitza et.at. [2]. Since R actually is the given parameter in our computations we have adjusted this parameter until the required value of $\bar{Q}_x$ was obtained. The surface deflection is given in terms of the quantity

$$\phi = \frac{\zeta_{max} - \zeta_{min}}{\zeta_{max} + \zeta_{min}}$$

where ζ_{max} and ζ_{min} denote respectively the maximum and minimum thickness of the fluid layer. The results are presented in Table 3.

Table 1

α	$B_1^{(s)}$	$B_2^{(s)}$	$B_3^{(s)}$	$\Delta_1^{(s)}$	$\Delta_2^{(s)}$	β_{1i}	c	ζ_{max}	ζ_{min}	$\overline{Q_x}$ cm^2/s
0.040	0.0202	-0.0023	0.0002	0.584	0.222	-1.995	-1.985	1.037	0.955	0.0761
0.037	0.0232	-0.0044	0.0004	0.659	0.249	-1.994	-1.976	1.041	0.945	0.0762
0.034	0.0219	-0.0053	0.0006	0.702	0.291	-1.993	-1.974	1.040	0.946	0.0761
0.030	0.0176	-0.0066	0.0009	0.721	0.404	-1.993	-1.971	1.032	0.951	0.0761

Table 2

α	$B_1^{(s)}$	$B_2^{(s)}$	$B_3^{(s)}$	$\Delta_1^{(s)}$	$\Delta_2^{(s)}$	β_{1i}	c	ζ_{max}	ζ_{min}	$\overline{Q_x}$ cm^2/s
0.069	0.0448	-0.0037	0.0003	1.316	0.687	-1.985	-1.972	1.088	0.908	0.0337
0.064	0.0598	-0.0087	0.0011	1.420	0.755	-1.980	-1.960	1.120	0.873	0.0340
0.059	0.0614	-0.0119	0.0017	1.489	0.834	-1.978	-1.960	1.126	0.867	0.0341
0.051	0.0526	-0.0160	0.0024	1.583	1.032	-1.978	-1.970	1.117	0.882	0.0339
0.042	0.0301	-0.0174	0.0027	1.654	1.286	-1.982	-1.986	1.083	0.916	0.0336

Table 3

Kapitza et al.'s observations							Computed values		
Liquid	ν cm^2/s	T/ρ cm^3/s^2	$\bar{Q}_x$ cm^2/s	λ cm	ϕ	c_s cm/s	R	ϕ	c_s cm/s
Water	0.0114	74	0.061	0.89	0.16	12.4	7.39	0.26	12.06
Alcohol	0.0202	29	0.068	0.71	0.18	10.7	4.63	0.27	10.64

It is seen from Table 3 that the computed wave velocities, c_s, agree well with the measured values reported by Ref. 2. But the computed values of ϕ are considerably higher than the measured values. Although the agreement is somewhat improved as compared to the results in (I) the discreapency is larger than the estimated error of the measurements given by Ref. 2. For the values of α and R treated in Table 3, however, higher order terms in LWE might have some influence on the equilibrium amplitudes. There is also another point which should be considered. The numerical results in § 5 show that for flow rates in the range where the onset of wave motion is reported, the downstream development of the wave train is very slow. Thus in experiments in this range of flow rates care must be taken in order to observe the actual steady far-field amplitude value.

5. Spatial variations of the wave trains.

In order to study the spatial variation of the wave trains we shall integrate (7a) and (7b) numerically and we shall apply the same method of integration as already described in (I). Consequently

we write

$$\tilde{A}_1 = B_1 e^{i\theta_1} , \tag{15a}$$

$$\hat{A}_2 = B_2 e^{i\theta_2} , \tag{15b}$$

$$\Delta_1 = \theta_2 - 2\theta_1 , \tag{15c}$$

where B_1, B_2, θ_2 and θ_2 are real functions of x. Thus by substitution of (15a) - (15c) in (7a) and (7b) four differential equations are obtained, namely; three equations for the variables B_1, B_2 and Δ_1 and a fourth equation describing θ_1, as function of x. The variation of θ_1 with x along the wave train will physically imply a variation of the wavelength in the downstream direction. For a wave train with a growing amplitude in the downstream direction it can be shown that the wavelength decreases slowly until it adjusts to its far-field limit, while for a decaying wave train, the wave length increases slowly in the downstream direction. It also becomes evident from (Eq.9) that for a spatially growing wave train the mean layer thickness decreases in the downstream direction while for a spatially decaying wave train the mean layer thickness increases.

If the values of B_1, B_2 and Δ_1 are described at the boundary station (see § 1) the surface deflection in the downstream direction can be found. The boundary conditions on B_1, B_2 and Δ_1 should match the disturbances introduced by the wave generator. If this is vibrating at a fixed frequency, c, these conditions might be modelled by the following conditions; B_1 corresponds to the amplitude of the fundamental frequency. However, B_2 and Δ_1 have values determined by the background noice. The downstream development of the wave train will therefore depend

on the boundary values of B_2 and Δ_1. For boundary values $|B_2| << |B_1|$ it is however found that except for values of x close to the boundary station the downstream development is almost independent of the boundary values imposed on B_2 and Δ_1.

Numerical results showing the spatial variation of the amplitude B_1 for a wave train on a water film are presented in the graphs in Figure 1 and 2. These computations are performed for two different angles of inclinations, namely $\theta = \frac{\pi}{24}$, $\theta = \frac{\pi}{2}$ and for values of the flow parameters in the range where the observed onset of wave motion is reported. (Refs. 2,3).

For a given frequency the amplitude B_1 is normalized by corresponding far-field amplitude $B_1^{(s)}$. However, for the damped wave trains the amplitude is normalized by the far-field amplitude correponding to $\alpha = 0.064$ (9.9 Hz) in the case of $\theta = \frac{\pi}{2}$ (Figure 1), and to the far-field amplitude corresponding to $\alpha = 0.040$ (2.1 Hz) in the case of $\theta = \frac{\pi}{24}$ (Figure 2).

For a water film falling on a vertical plane Figure 1 shows that in the frequency range from 9.9 Hz to 8.0 Hz a periodic perturbation will adjust relatively rapidly to its far-field value. For boundary perturbations of magnitude half the far-field value the adjustment will occur over a distance of approximately 20 wavelengths while for boundary perturbations of magnitude one tenth of the far-field value the adjustment distance is approximately 40 wavelengths. For frequencies closer to linear neutral conditions (10.8 Hz) the adjustment to the far-field value is very slow. For frequencies above 13.7 Hz a perturbation is rapidly damped and its amplitude is vanishingly small at a distance of 20 wavelengths from the boundary station. (For frequencies somewhat

lower than 8.0 Hz, β_{2r} tends to zero, and obviously in this range of frequencies several terms in the expansion (5) must be retained in order to establish an eventual steady far-field wave solution.)

The data for the case $\theta = \frac{\pi}{24}$ reveal generally the same dependence on the frequency. But even the volume flux is higher in this case the downstream variation of the wave trains is much slower. This is to be expected since on a slightly inclined plane the available potential energy for the perturbation motion will be less. It is seen from Figure 2 that with perturbations at the boundary station of magnitude one half of the corresponding far-field values, the adjustment to this latter amplitude will only occur at a distance of at least 100 wavelengths in the downstream direction.

Observations of forced wave trains on liquid films are scarce. To our knowledge Koehler [3] is the only author who gives a qualitative description of the spatial variation of forced wave trains. Koehler's observations are made on a slightly inclined plane. Our computations for the case $\theta = \frac{\pi}{24}$ seem to agree with these observations. It is regretable that no quantitative measurements exist so that a direct comparison between theory and experiments can be made.

Appendix

The functions introduced in Eq (4) are defined by

$$A(\zeta) = \tfrac{2}{3}\,\zeta^3$$

$$B(\zeta) = \tfrac{8}{15}\,R\zeta^6 - \tfrac{2}{3}\cot\theta\zeta^3$$

$$C(\zeta) = \tfrac{2}{3}\,\alpha^2 W\zeta^3$$

$$D(\zeta) = \tfrac{1016}{315}\,R^2\zeta^9 + \tfrac{14}{3}\,\zeta^3 - \tfrac{32}{15}\,R\cot\theta\zeta^6$$

$$E(\zeta) = \tfrac{32}{63}\,R^2\zeta^{10} + 2\zeta^4 - \tfrac{40}{63}\,R\cot\theta\zeta^7$$

$$F(\zeta) = \tfrac{40}{63}\,\alpha^2 RW\zeta^7$$

$$G(\zeta) = \tfrac{16}{3}\,\alpha^2 RW\zeta^6$$

$$H(\zeta) = \tfrac{16}{5}\,\alpha^2 RW\zeta^6$$

$$I(\zeta) = \tfrac{32}{5}\,\alpha^2 RW\zeta^5\ ,$$

while the coefficients in (7a) and (7b) are

$$\beta_k = \alpha k^2[B(1) - k^2C(1)]$$
$$+ i[-kA'(1) + \alpha^2k^3(E(1) - k^2F(1))]\ ,\quad (k = 1,2)\ ,$$

$$p = 2\alpha[B'(1) - C'(1)]$$
$$+ i[-A''(1) + 2\alpha^2(D(1) + E'(1) - F'(1) - G(1) - H(1))]\ ,$$

$$q = \alpha[B'(1) - 7C'(1)]$$
$$+ i[-A''(1) + \alpha^2(-4D(1) + 5E'(1) - 17F'(1) + 10G(1) - 8H(1)]\ ,$$

$$m = \frac{\alpha}{2}[B''(1) - C''(1)]$$

$$+ i[-\tfrac{1}{2} A'''(1) + \alpha^2(-D'(1) + \tfrac{3}{2} E''(1) - \tfrac{3}{2} F''(1) + G'(1) - 3H'(1) + 3I(1))]$$

$$a_1 = A'(1) - \alpha^2[3E(1) - 5F(1)] + i2\alpha[B(1) - C(1)] ,$$

$$a_2 = A'(1) - 4\alpha^2[3E(1) - 20F(1)] + i4\alpha[B(1) - 8C(1)] ,$$

$$r = \alpha[B'(1) - C'(1)] + i[- A''(1) + \alpha^2(E'(1) - F'(1))] ,$$

where prime denotes differensiation with respect to ζ.

Footnotes

1) Gjevik, B. Phys. Fluids, 13, 1918 (1970).

2) Kapitza, P.L. & Kapitza, S.P. Zh. Eksp. Teor. Fiz 19, 105 (1949).

3) Koehler, R. Dissertation. Georg-August-Universität, Göttingen, Germany (1968).

4) Lin, S.P. Phys. Fluids, 10, 308 (1967).

5) Eckhaus, W. Studies in Non-linear Stability Theory. Chp. 8. Berlin. Springer.

6) Benney, D.J. J. Math. and Phys. XLV, 150 (1966).

7) Lin, S.P. J. Fluid Mech., 40, 307 (1970).

Table and Figure Captions

Table 1 Data for steady finite-amplitude surface waves (far-field waves) on a water film with $\theta = \frac{\pi}{24}$, $R = 11.39$ and $W = 859$.

Table 2 Data for steady finite-amplitude surface waves (far-field waves) on a water film with $\theta = \frac{\pi}{2}$, $R = 5.0$ and $W = 755$.

Figure 1 Spatial variation of the ratio $B_1/B_1^{(s)}$ at $R = 5$ ($\bar{Q}_x \cong 0.034$ cm^2/s), $\theta = \frac{\pi}{2}$, and $W = 755$ (water) for different values of the frequency and for two different boundary conditions. ($B_1/B_1^{(s)} = 0.5$ og 0.1).
Curve I: 10.8 Hz ($\alpha = 0.069$). Curve II: 9.9 Hz ($\alpha = 0.064$).
Curve III: 9.2 Hz ($\alpha = 0.059$). Curve IV: 8.0 Hz ($\alpha = 0.051$).
Damped wave trains (dotted lines) curves V,VI, and VII for 12.1 Hz, 13.7 Hz, and 16.2 Hz respectively. (For these curves B_1 is normalized by the value of $B_1^{(s)}$ corresponding to 9.9 Hz.

Figure 2 Spatial variation of the ratio $B_1/B_1^{(s)}$ at $R = 11.39$ ($\bar{Q}_x \cong 0.076$ cm^2/s), $\theta = \frac{\pi}{24}$, and $W = 859$ (water) for different values of the frequency and for two different boundary conditions ($B_1/B_1^{(s)} = 0.5$ or 0.1).
Curve I: 2.1 Hz ($\alpha = 0.040$). Curve II: 1.9 Hz ($\alpha = 0.037$
Curve III: 1.8 Hz ($\alpha = 0.034$).Damped wave trains (dotted lines) curves IV, V, and VI for 2.3 Hz, 2.6 Hz, and 3.1 Hz respectively (For these curves B_1 is normalized by the value of $B_1^{(s)}$ corresponding to 2.8 Hz.)

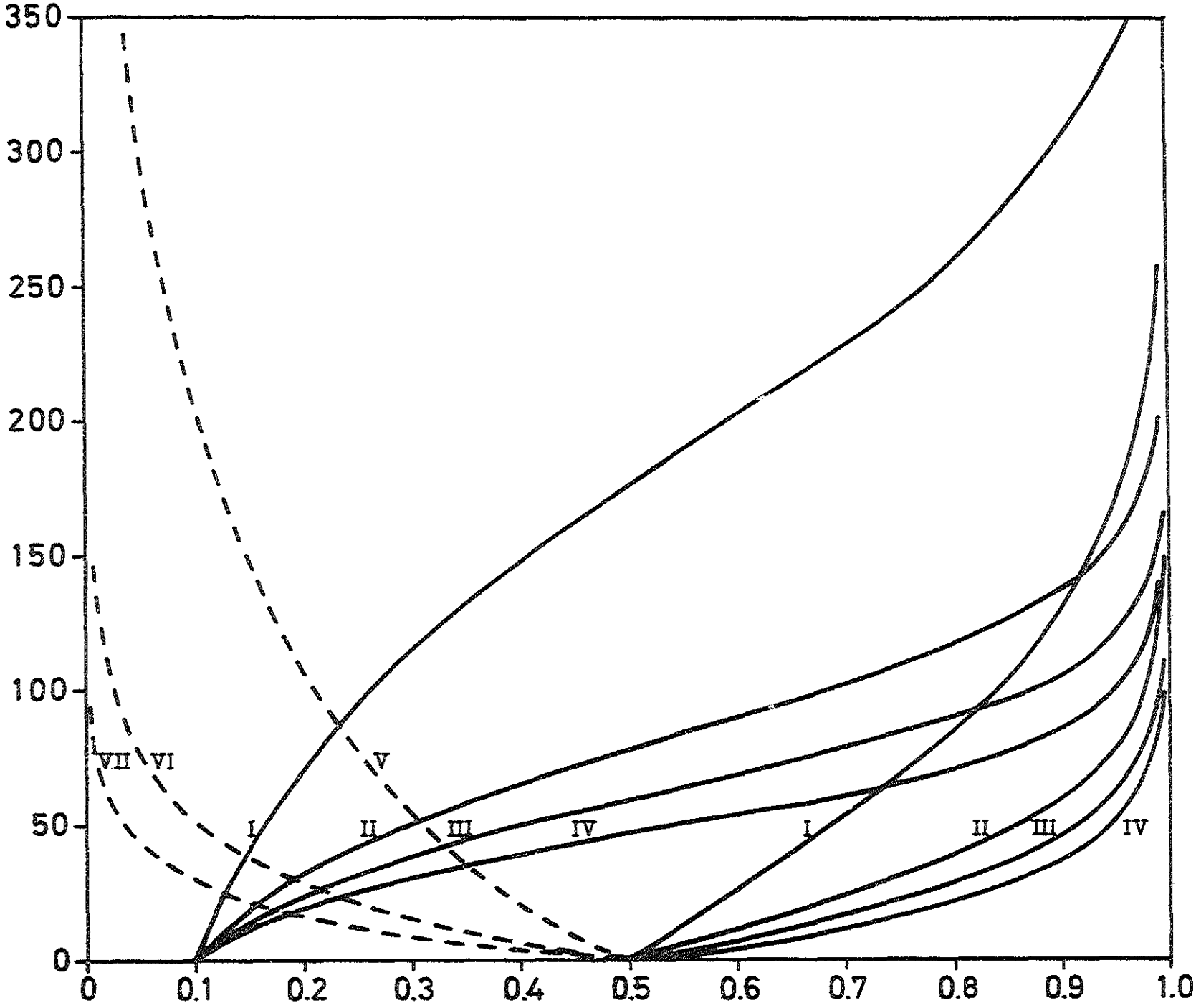
350
300
250
200
150
100
50
0
0
0.1
0.2
0.3
0.4
0.5
0.6
0.7
0.8
0.9
1.0
VII
VI
V
I
II
III
IV
I
II
III
IV

Figure 1

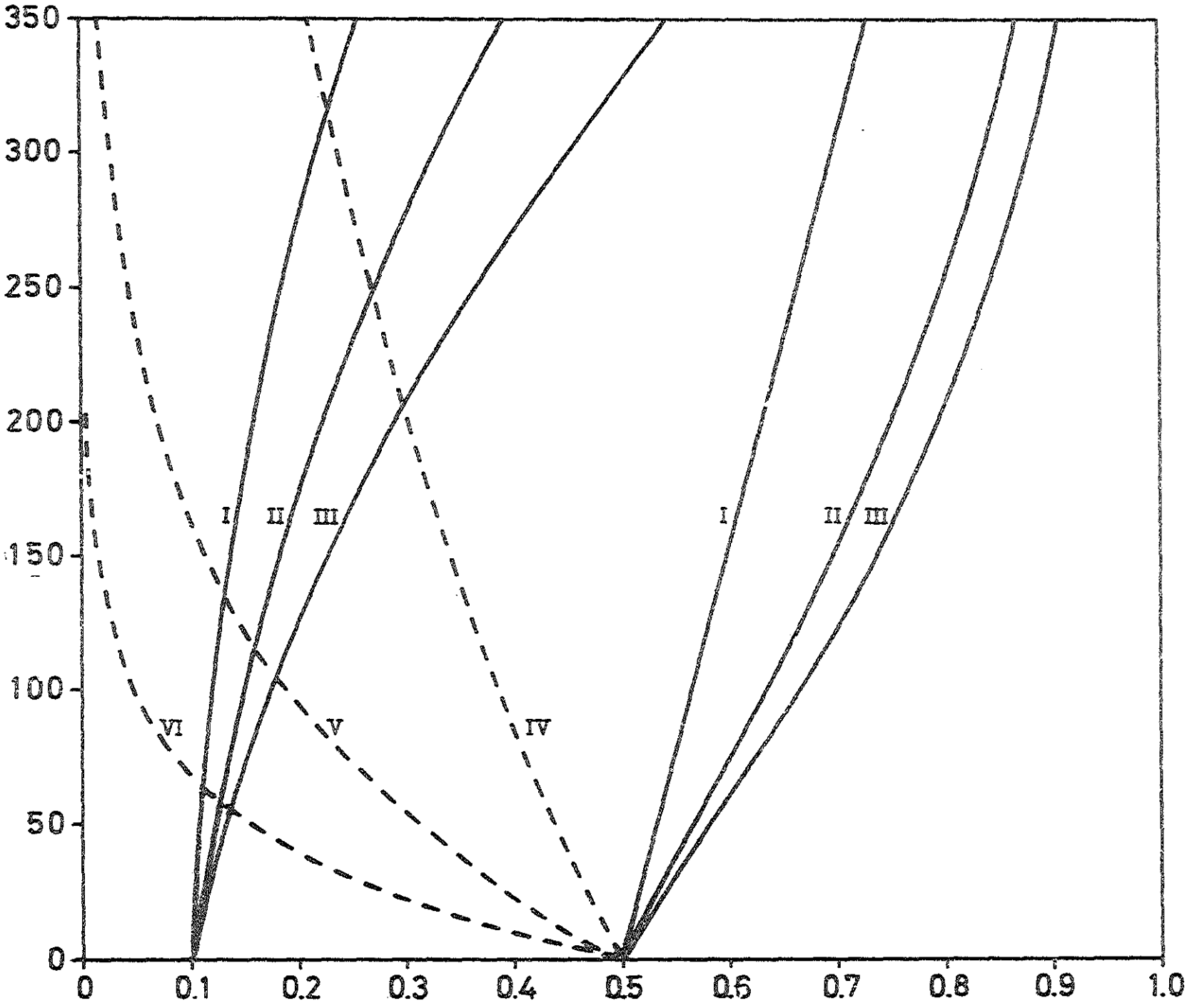
350
300
250
200
150
100
50
0
0
0.1
0.2
0.3
0.4
0.5
0.6
0.7
0.8
0.9
1.0
I
II
III
IV
V
VI
I
II
III

Figure 2